

Dual-color Proteomic Profiling of Complex Samples with a Microarray of 810 Cancer-related Antibodies*[§]

Christoph Schröder^{‡§}, Anette Jacob[‡], Sarah Tonack[¶], Tomasz P. Radon^{||}, Martin Sill^{**}, Manuela Zucknick^{**}, Sven Ruffer[‡], Eithne Costello[¶], John P. Neoptolemos[¶], Tatjana Crnogorac-Jurcevic^{||}, Andrea Bauer[‡], Kurt Fellenberg^{††}, and Jörg D. Hoheisel[‡]

Antibody microarrays have the potential to enable comprehensive proteomic analysis of small amounts of sample material. Here, protocols are presented for the production, quality assessment, and reproducible application of antibody microarrays in a two-color mode with an array of 1,800 features, representing 810 antibodies that were directed at 741 cancer-related proteins. In addition to measures of array quality, we implemented indicators for the accuracy and significance of dual-color detection. Dual-color measurements outperform a single-color approach concerning assay reproducibility and discriminative power. In the analysis of serum samples, depletion of high-abundance proteins did not improve technical assay quality. On the contrary, depletion introduced a strong bias in protein representation. In an initial study, we demonstrated the applicability of the protocols to proteins derived from urine samples. We identified differences between urine samples from pancreatic cancer patients and healthy subjects and between sexes. This study demonstrates that biomedically relevant data can be produced. As demonstrated by the thorough quality analysis, the dual-color antibody array approach proved to be competitive with other proteomic techniques and comparable in performance to transcriptional microarray analyses. *Molecular & Cellular Proteomics* 9: 1271–1280, 2010.

Proteomic studies are essential for elucidating the molecular mechanisms involved in cellular functioning as well as

From the Divisions of [‡]Functional Genome Analysis and ^{**}Division of Biostatistics, Deutsches Krebsforschungszentrum, 69120 Heidelberg, Germany; [¶]Division of Surgery and Oncology, University of Liverpool, Liverpool L69 3GA, United Kingdom; ^{||}Barts and The London School of Medicine and Dentistry, Queen Mary University of London, Centre for Molecular Oncology and Imaging, Institute of Cancer, London EC1M 6BQ, United Kingdom; ^{††}Chair of Bioanalytics, Centre for Integrated Protein Sciences Munich, Technical University Munich, 85354 Freising, Germany

* Author's Choice—Final version full access.

Received September 5, 2009, and in revised form February 12, 2010.

Published, MCP Papers in Press, February 16, 2010, DOI 10.1074/mcp.M900419-MCP200

disease development and progression. For cancer, proteomic techniques may pave the way for the identification of therapeutic targets and provide new diagnostic modalities, facilitating an early detection of cancer onset (1, 2). Moreover, such studies could contribute more detailed information on the characteristics of a patient's tumor (3), which is critical for a more successful treatment. At first, however, panels of biomarker molecules must be established and validated in a clinical setting. In this respect, the currently established proteomic technologies have only limited success (4–7). This might be due in part to the challenge of translating proteomic findings, which are currently largely obtained by mass spectrometry methods, into immunodiagnostic assays, which are the preferred format in clinical laboratories (5). Another limitation is the lack of capacity for a simultaneous assessment of a very large variety of potential biomarkers in a high number of samples. As an immuno-based, high-throughput technique, antibody microarrays could provide a solution (8–10). In principle, they allow the detection of an almost unlimited number of analytes in a parallel format from very small sample volumes, with a sensitivity that is in the picomolar to femtomolar range even without signal amplification (11, 12). This sensitivity is similar to that achievable with ELISA, the “gold standard” for protein quantification.

One current drawback of the technology, different from mass spectrometry, is the fact that the analytes have to be defined in advance. Although this has limited the application of antibody microarrays for biomarker discovery in the past, the advent of more comprehensive microarrays increases their suitability. The constantly growing numbers of tested antibodies will facilitate profiling studies, which will provide a better understanding of protein regulation in human disease and in turn enhance the probability of detecting prognostic or diagnostic markers.

However, as with DNA microarrays for transcript profiling, several technical improvements are essential to achieve similarly accurate results (13). In this report, we describe processes that were applied successfully in the production of more than 1,000 arrays, each comprising a comparably large number of 1,800 features. To ensure a high homogeneity

among these arrays and the features within each array, production protocols were adapted and quality controls implemented. The impact of measurements in a dual-color mode on assay robustness as well as differentiation power was assessed, and relevant parameters, such as the concordance of the two color channels, were carefully validated. With the established protocols, the necessity of serum depletion for antibody microarray measurements was investigated. In addition to plasma and serum samples, the robust applicability to proteins extracted from human urine samples was demonstrated in a preliminary study on pancreatic cancer.

EXPERIMENTAL PROCEDURES

Antibodies—Targets exhibiting differential expression were selected from transcriptional studies on different cancer entities (14–16). For 668 of these targets, affinity-purified, peptide-specific, polyclonal antibodies from rabbit were provided by Eurogentec (Seraing, Belgium). An additional 142 antibodies were purchased from different companies or provided by collaborating partners. Antibodies supplied as ascites fluid, antisera, or with stabilizer proteins were purified using the NAb Protein G Spin Kit (Thermo Fisher Scientific, Waltham, USA). The concentration of all antibodies was adjusted to 2 mg/ml by filtration with Microcon 100 kDa (Millipore, Schwalbach, Germany) before aliquoting and storage at -80°C .

Array Production—All antibodies were diluted in $2\times$ spotting buffer (20 mM sodium borate buffer, pH 9.0, 250 mM MgCl_2 , 0.01% (w/v) sodium azide, 0.5% (w/v) dextran, and 0.001% (w/v) [octylphenoxypolyethoxyethanol in distilled water) and printed on epoxysilane slides (Schott Nexterion, Jena, Germany) with a Microgrid microarraying robot (BioRobotics, Cambridge, UK) using SMP3B pins (Telechem, Sunnyvale, CA) to have $10\ \mu\text{l}$ of a 1 mg/ml antibody solution. Thereby $10\ \mu\text{g}$ of each antibody were used for the production of more than 1000 microarrays, which is approximately 100 times less than required for 1000 ELISA wells using standard procedures. All antibodies were spotted twice in a randomized pattern in different array sectors. In addition, commercial monoclonal antibodies against particular cancer-related proteins were added in duplicates. Antibodies against the proteins β -actin (ACTB),¹ human IgM, glyceraldehyde-3-phosphatase dehydrogenase, and against albumin were spotted as housekeeping controls. For the same purpose, a polyclonal antibody directed against whole human serum protein was added. Negative controls consisting of only a spotting buffer were added as well as further control antibodies (e.g. molecules directed against mouse immunoglobulin gamma). All these controls were spotted in 8 to 18 copies across the entire array to ensure a good distribution of the controls for eventual normalization purposes. After printing, slides were kept at 4°C overnight, washed 10 times with 0.05% (w/v) Tween 20 and 0.05% (w/v) Triton X-100 in PBS and blocked in 4% (w/v) nonfat dry milk and 0.05% (w/v) Tween 20 in PBS overnight. After blocking, slides were washed four times with PBS/Tween 20/Triton X-100, twice with $0.1\times$ PBS, and dried by an air stream before storage in a humidity chamber at 4°C for up to 1 year.

Quality Control of Array Production—To control antibody immobilization on the microarray surface, a representative portion of slides from each production batch was stained with Sypro Ruby (Fig. 1b). Slides were washed thoroughly with PBS/Tween 20/Triton X-100

instead of performing blocking. Subsequently, they were submerged with the ready-to-use Sypro Ruby staining solution (Sigma-Aldrich) for 1 h. After staining, the slides were washed four times with 10% methanol and 7% acetic acid in H_2O . After rinsing twice with water, slides were dried in an air stream. Images were recorded with a Packard ScanArray 4000XL scanner (PerkinElmer Life and Analytical Sciences) at excitation and emission wavelengths of 450 and 610 nm, respectively.

In addition, part of the slides was incubated for 2 h in blocking buffer with 5 nM secondary antibodies that were directed against rabbit IgG or mouse IgG (Jackson ImmunoResearch Laboratories, Suffolk, UK) and conjugated with the fluorescent dyes Cy3 or Cy5, respectively (Fig. 1c). Sample incubation and washing procedures were done as with complex protein samples.

Sample Preparation—All serum, plasma and urine samples were collected with the informed consent and with full ethical approval from the host institutions. For a technical assessment (Figs. 1d and 3), three blood plasma samples from healthy donors were pooled. For plasma and serum samples, the protein concentration was measured by the bicinchoninic acid (BCA) assay (Thermo Fisher Scientific); for urine samples, the Bradford assay (Coomassie Protein Assay Reagent; Thermo Fisher Scientific) was used.

Serum Depletion—After delipidization (17), a serum sample was split in two parts. While one part served as a nondepleted control, the other was used for immunodepletion with the ProteoPrep[®] 20 Plasma Immunodepletion kit (Sigma-Aldrich) as described previously (18). The kit removes 20 highly abundant proteins by antibodies immobilized on agarose beads. Delipidated serum ($200\ \mu\text{l}$) was diluted in 2 ml of equilibration buffer (included in the kit) and cleared from residual particles by centrifugation through $0.2\text{-}\mu\text{m}$ spin filter columns. For depletion, the diluted serum was added to the equilibrated depletion column in 20 steps of $100\ \mu\text{l}$ each and incubated for 15 min; the column was spun at $2000\times g$ for 30 s. Proteins bound to the column were eluted, and the column was re-equilibrated for further usage. The 20 fractions were combined and concentrated to $200\ \mu\text{l}$ using Microsep 1K centrifugal devices (Pall Life Science, Portsmouth, UK) before an additional final depletion step, as recommended by the manufacturer. To control depletion efficiency, samples were analyzed by SDS-PAGE. For buffer exchange, the depleted sample was diluted in 2 ml of PBS and concentrated with Microsep 1K centrifugal devices at $7,500\times g$ to a volume of less than $100\ \mu\text{l}$.

Preparation of Urine Proteins—Midstream urine samples were collected from 12 subjects and pH was adjusted to 7. The samples were desalted and concentrated as described in detail elsewhere (19). In brief, samples were desalted using Zeba spin columns (Thermo Fisher Scientific). The flow-through was frozen in liquid nitrogen and lyophilized to dryness using a freeze dryer (Ilmvac, Ilmenau, Germany). Lyophilized samples were resolubilized in distilled water and concentrated with Vivaspin 15R-5 kDa (Sartorius Vivascience, Hannover, Germany).

Sample Labeling—Plasma, serum, and urine samples were labeled at a protein concentration of 4 mg/ml with 0.4 mg/ml of the *N*-hydroxysuccinimide esters of the fluorescence dyes Dy-549 or Dy-649 (Dyomics, Jena, Germany) in 100 mM sodium bicarbonate buffer, pH 9.0, 1% (w/v) Triton X-100 on a shaker at 4°C . After 1 h, the reactions were stopped by addition of hydroxylamine to 1 M. Unreacted dye was removed 30 min later, and the buffer was changed to PBS using Zeba Desalt columns (Thermo Scientific). Subsequently, Complete Protease Inhibitor Mixture tablets (Roche) were added as recommended by the manufacturer. Labeled samples were either incubated directly or stored in aliquots at -20°C .

Incubation—Custom incubation chambers were attached to the array slides with Terostat-81 (Henkel, Düsseldorf, Germany). The inner dimensions of the incubation chambers matched the area of

¹ The abbreviations used are: ACTB, β -actin; SNR, signal-to-noise ratio; CV, coefficient of variation; LIMMA, linear models for microarray data; KLK3, Kallikrein-3; M-CHiPS, multiconditional hybridization intensity processing system.

the array (9 × 18 mm) with an additional border of 2 mm and a height of 5 mm. Before adding the labeled protein samples, the arrays were blocked in a casein-based blocking solution (Candor Biosciences, Weißensberg, Germany) on a Slidebooster instrument (Advalytix, Munich, Germany) for 3 h. Incubation was performed with labeled samples diluted 1:20 in blocking solution containing 1% (w/v) Tween 20 and Complete Protease Inhibitor Mixture for 15 h in a total volume of 600 μ l. Slides were thoroughly washed with PBS/Tween 20/Triton X-100 before and after detaching the incubation chambers. Finally, the slides were rinsed with 0.1 × PBS and distilled water and dried in a stream of air.

Data Analysis and Statistical Testing—Slide scanning was done on a ScanArray 5000 or 4000XL unit using the identical instrument laser power and photomultiplier intensity in each experiment. Spot segmentation was performed with GenePix Pro 6.0 (Molecular Devices, Sunnyvale, CA). Resulting data were analyzed using the linear models for microarray data (LIMMA) package (20) of R-BioConductor after uploading the mean signal and median background intensities. For quality assessment (Fig. 3), slides were neither background-corrected nor normalized. In the depletion experiment and the urine profiling, the array results were background-corrected using the Normexp method (21) with an offset of 50. For the depletion experiment with a high percentage of differentially abundant proteins, an invariant Lowess normalization was applied (supplemental Methods). The urine profiling experiment was normalized with global Lowess (22). In the analyses, duplicate spots were accounted for (23); control spots as well as signals for anti-ACTB were removed. For differential analyses of the depletion experiment and the urine experiment, one-factorial and two-factorial linear models, respectively, were fitted with LIMMA, resulting in a two-sided *t* test or F-test based on moderated statistics. All presented *p* values were adjusted for multiple testing by controlling the false discovery rate according to Benjamini and Hochberg (24).

In the M-CHiPS (25, 26) analyses (Figs. 4d and 5a), the mean signal intensity of each spot without background subtraction was used, and data were normalized by log-linear regression. Tracking controls and anti-ACTB were not considered. In the plots, only proteins are shown, which exhibited significant variations ($p < 0.05$).

Pearson's correlation factors or coefficients of variation were averaged by their means. Signal-to-noise ratios (SNRs) were calculated by dividing the difference of signal and background intensity by the standard deviation of the background.

In the box plots (Figs. 2, 3c, and 4a), each box represents 50% of the data points. The median is represented as a line within the box. The whiskers extend to the most extreme data point, which is no more distant than 1.5 times the interquartile range. All outlying data points are depicted as dots.

RESULTS

Array Production—For large-scale proteomic studies of cancer samples, we constructed an antibody microarray of 810 polyclonal antibodies, targeting proteins encoded by genes that were selected mainly on the basis of variations in transcript levels observed in pancreatic (14, 15) and colon cancer (16). All antibodies were spotted twice in different array sectors. In addition, commercial monoclonal antibodies against particular cancer-related and housekeeping proteins were added, the latter in 8–18 copies each, spots without protein (negative controls), as well as two-color tracking spots that indicate slide orientation and offer a standard for color detection (Fig. 1a). In total, the array comprised 1,800 features. To obtain a sufficiently large number of arrays for sta-

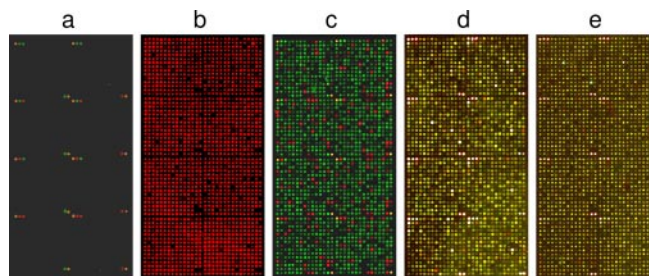


FIG. 1. Quality control measures for an antibody microarray of 1,800 features. a, two-color positional controls facilitate grid tracking, slide orientation and support the verification of spot segmentation. They also serve as color standards during the imaging process. b, Sypro Ruby staining of all proteins acts as a quality measure of antibody immobilization. Negative control spots show no immobilized protein. c, incubation with 5 nM concentrations of each fluorescently labeled antibody against rabbit IgG (green signals) and mouse IgG (red) confirmed that the majority of antibodies on the microarray were produced in rabbits. Some antibodies, which were stained by Sypro Ruby but not in the incubation with secondary antibodies, were produced in goat or hamster. d, fluorescence image of a microarray incubated with two plasma samples of healthy donors for array quality control. One sample was labeled with the dye Dy-549, the other with dye Dy-649 before a competitive incubation in a dual-color mode. e, fluorescence image of a representative array of the analysis of urine samples from patients with pancreatic cancer. A urine sample and a reference consisting of a pool of samples from diseased and healthy subjects were labeled with different fluorescent dyes and incubated on the array in a competitive dual-color assay.

tistically significant studies, we produced 540 slides in five successive batches from the same set of source plates that held the antibodies. On each slide, two separate but identical arrays were spotted. Therefore, a total of 1,080 arrays were produced for individual incubations.

As a quality control of the production process, slides from each batch were stained with the fluorescent dye Sypro Ruby (Fig. 1b) or incubated simultaneously with two secondary antibodies directed against mouse or rabbit IgG and labeled with Cy5 or Cy3, respectively (Fig. 1c). The latter analysis clearly identified the host of antibody production. This result and the lack of signals from the negative control spots demonstrated that carry-over effects during the production process had been prevented effectively. In addition, both tests indicated the high degree of pattern homogeneity among the slides. In the experiments with the secondary antibodies, a correlation coefficient of at least 0.92 was obtained for slides of the same production batch and a value of more than 0.86 for arrays from different production batches. In addition, highly consistent signal patterns could be obtained from experiments with complex protein samples. Part of the slides was incubated with complex plasma samples in a dual-color mode for quality control purposes. Two plasma samples of healthy donors were labeled by the fluorescent dyes Dy-549 and Dy-649 and incubated competitively in a dual-color assay (Fig. 1d). Incubations with protein samples derived from human urine led, on average, to similar signal and background intensity levels (Fig. 1e).

Advantage of Dual-Color to One-Color Measurements—In transcriptional studies with custom DNA microarrays, mainly dual-color assays are performed because of the improved assay robustness. To determine whether this is also true for antibody microarray assays, one-color and dual-color mode measurements were compared. Two protein samples (A and B) were labeled with the fluorescent dye Dy-549. In addition, a pool of plasma samples was labeled with Dy-649 as a common reference for the measurements in dual-color mode. Sample A was incubated on three different microarrays and sample B on two different microarrays in a one-color assay. In addition, they were incubated in a competitive manner with the reference sample in dual-color mode. The raw signal intensities of the one-color assay were compared with the ratios of the two color channels of the dual-color measurements. For all array features except positional and negative controls, the coefficients of variation (CV) were calculated on the interarray replicates as well as the intra-array spot duplicates, six values of sample A and four measurements of sample B per antibody. In addition, the CV was calculated for all 10 measurements of samples A and B. For both samples, the average CV as well as the complete distribution of CV values was significantly lower for the dual-color mode measurements (Fig. 2a). This demonstrates the superior performance of dual-color mode measurements regarding the assay robustness. In addition, higher CV were obtained on average for the combined calculation of samples A and B in the dual-color mode. This is expected, because the combination of two samples adds biological variability to the data. However, this could not be observed for both samples in the one-color analysis, indicating that slight differences between two samples can be more easily recorded using a dual-color measurement mode. To confirm this finding, the data were subjected to hierarchical cluster analysis using Euclidian distance and the complete-linkage algorithm (Fig. 2b). Also in this analysis, measurements in a dual-color mode outperformed a one-color analysis.

Assay Quality Indicators for Dual-color Measurements—To evaluate assay reliability, a plasma sample pool was labeled with the fluorescent dyes Dy-549 and Dy-649, respectively, and incubated in a dual-color assay on four arrays of each of the five batches, two each from the beginning and end of a production run. We assessed dye-specific effects by the Pearson's correlation coefficient (r) of the two color signal intensities of each array. Without filtering, we obtained on average $r = 0.93$ on all 20 arrays with $0.89 \leq r \leq 0.96$ (Fig. 3a, supplemental Fig. 1). Only one protein (ACTB) exhibited a dye bias and was therefore not considered in subsequent analyses.

As an indicator of assay reproducibility, we calculated the interarray CVs for all 1,800 array features without any filtering on the ratios of the two color signals (Fig. 3b). For 20 slides derived from the five production batches, the average (mean) CV was 13%, ranging from 9 to 14%. We obtained a CV

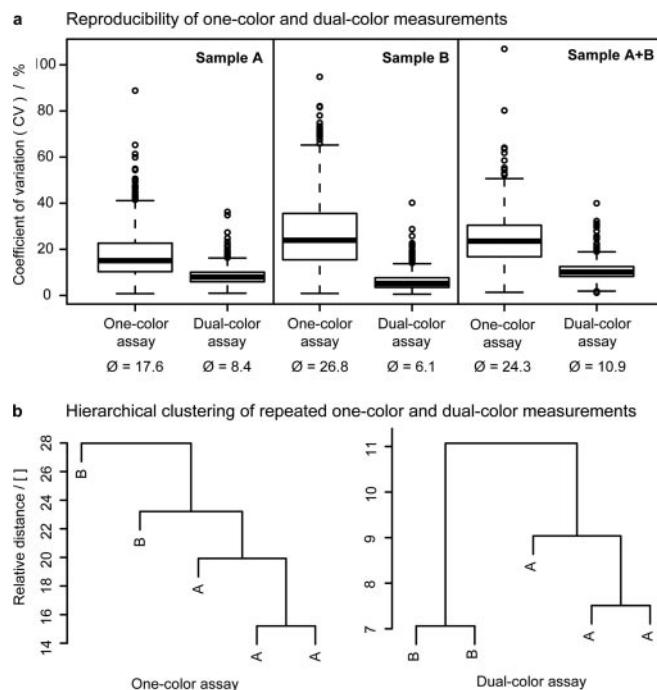


FIG. 2. Comparison of the assay robustness and differentiation power of one-color and dual-color mode experiments. *a*, two plasma samples (*Sample A*, *Sample B*) were labeled with the fluorescent dye Dy-549 and incubated in one-color and dual-color assays. CVs were calculated for 6 (*Sample A*), 4 (*Sample B*), or 10 (*Sample A + B*) replicate measurements derived from two, three, and five microarrays and their intra-array duplicates. Each box plot represents 872 data points that correspond to all array features besides positional and negative controls. CV were significantly lower for dual-color mode measurements of the two samples. The combination of both samples leads to increased CV for the dual-color but not for the one-color measurements. The increase (expected because of biological variability) indicates a better discriminative power of the dual-color approach. *b*, discriminative power of the two measurement modes was assessed by hierarchical clustering of the nonnormalized and non-log-transformed data. For dual-color measurements, repeated measurements of the samples on different microarrays clustered better, leading to a superior differentiation of the two samples.

<15% for 89% of all array features and a CV <20% for 96% of the features.

To examine the concentration differences that can be recorded in a complex sample, we labeled a plasma sample pool with different dyes and mixed the two fractions before incubation in different ratios ranging from 250:1 to 1:250. The ratios of the signal intensities obtained correlated well with the actual plasma ratios used in the incubations (Fig. 3c). As expected, and consistent with results on DNA microarrays, the plotted data form a sigmoid curve, with larger signal differences detectable at smaller ratios; even small variations could be clearly detected.

Depletion of High-abundance Proteins from Blood Is Not Necessary—In many proteomic studies, plasma or serum samples are depleted of abundant proteins such as albumin or immunoglobulins to increase the sensitivity for low-abun-

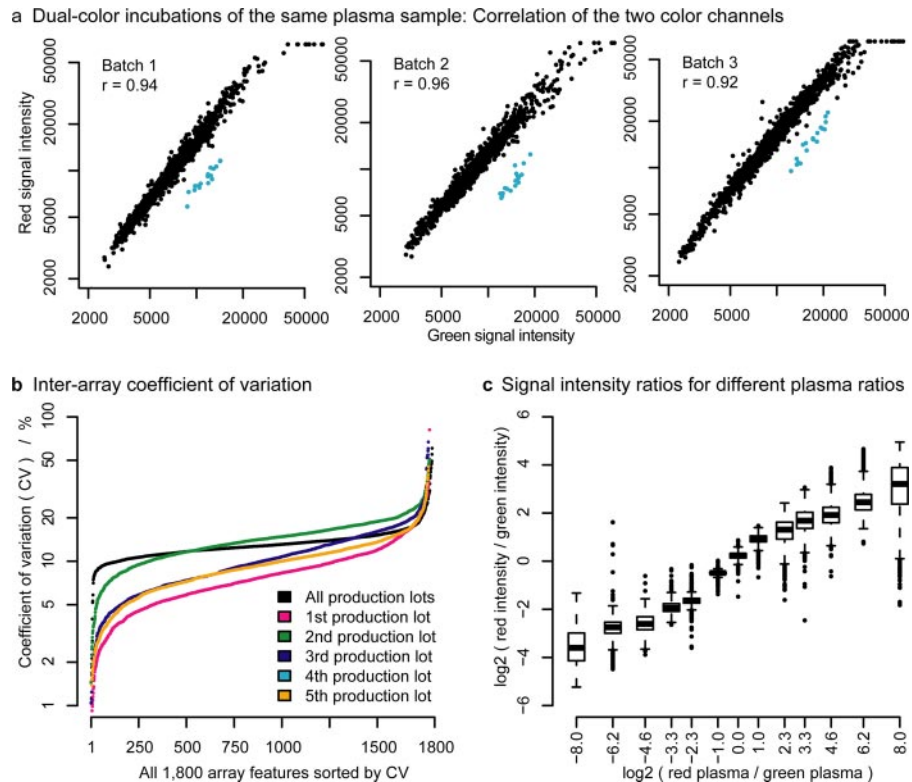


FIG. 3. Assay robustness of dual-color experiments on antibody microarrays. The same plasma sample was labeled with two different fluorescent dyes and incubated on the same slide. *a*, in the scatter plots, correlation of the red and green signal intensities of all array features ($n = 1,744$, tracking controls and negative controls excluded) are shown for three representative arrays. For the whole set of 20 microarrays, the average Pearson's correlation coefficient was 0.93. Only one protein, ACTB, captured by 18 antibody replicates (blue dots), exhibited significant differences. *b*, distribution of the CVs of the 1,800 array features. CVs were calculated for the ratios of red and green signal intensities. Each colored line represents the CVs for four arrays of the same production batch. The mean values ranged from 9 to 14% within production batches and 13% (black line) for all production batches combined. *c*, measurement accuracy of complex samples: a plasma sample was labeled with two fluorescent dyes in separate reactions and mixed in different ratios. After incubation, the ratios of the signal intensities show good correlation with the defined ratios of the plasma mixtures.

dance proteins. To evaluate the impact of protein depletion on the sensitivity of our antibody platform, we compared serum before and after depletion of 20 high-abundance proteins. The depleted and nondepleted samples were labeled with either Dy-549 or Dy-649, using the same amount of total protein. Each sample was incubated competitively with a common reference in a dual-color mode. The reference was made by a pool of the two serum sample types. Five incubations were done for each sample, also including dye swaps. As a measure of sensitivity, we calculated the SNR for both color channels and all antibody features (except anti-ACTB). Depletion was not accompanied by an increased SNR over the entire protein set. Likewise, when a random selection of 15 low-abundance cytokines was analyzed, no increase in SNR was observed (Fig. 4a).

Besides the impact of serum depletion on the assay performance in general, we investigated its impact on each protein with the LIMMA package (20) of R-BioConductor. Analysis revealed that a large set of 196 proteins (corresponding to 26% of the analyzed proteins) was affected by depletion at a significance level of $p < 0.05$ (Fig. 4b; supplemental Table 1).

Of these, 86 proteins were detected with higher intensities and 110 with lower intensities after depletion. The strongest enrichment was observed for CRP ($p = 10^{-10}$; supplemental Fig. 2a) followed by proteins such as TNF10, SORL, or TR10D (Fig. 4c). Cross-binding effects of albumin were excluded by an incubation of labeled human serum albumin on a different array at identical settings (data not shown). It is noteworthy that a control antibody directed against mouse-IgG also showed increased signal intensity in the depleted sample ($p = 3 \times 10^{-4}$; supplemental Fig. 2b). This may be due to a leakage of mouse antibodies from the column used in the protein depletion process. In addition to albumin ($10^{-5} < p < 7 \times 10^{-11}$; supplemental Fig. 2c), 109 rather than the expected 19 proteins other than albumin showed lower signal intensities after depletion, including FGF1 ($p = 10^{-8}$; supplemental Fig. 2d), SEPR, MLP3B and MAD4 (Fig. 4c), indicating codepletion effects.

We also analyzed the data by the M-CHiPS software package (25, 26). It handles filtering, background subtraction, and normalization differently from LIMMA and applies correspondence analysis for visualization. In the resulting

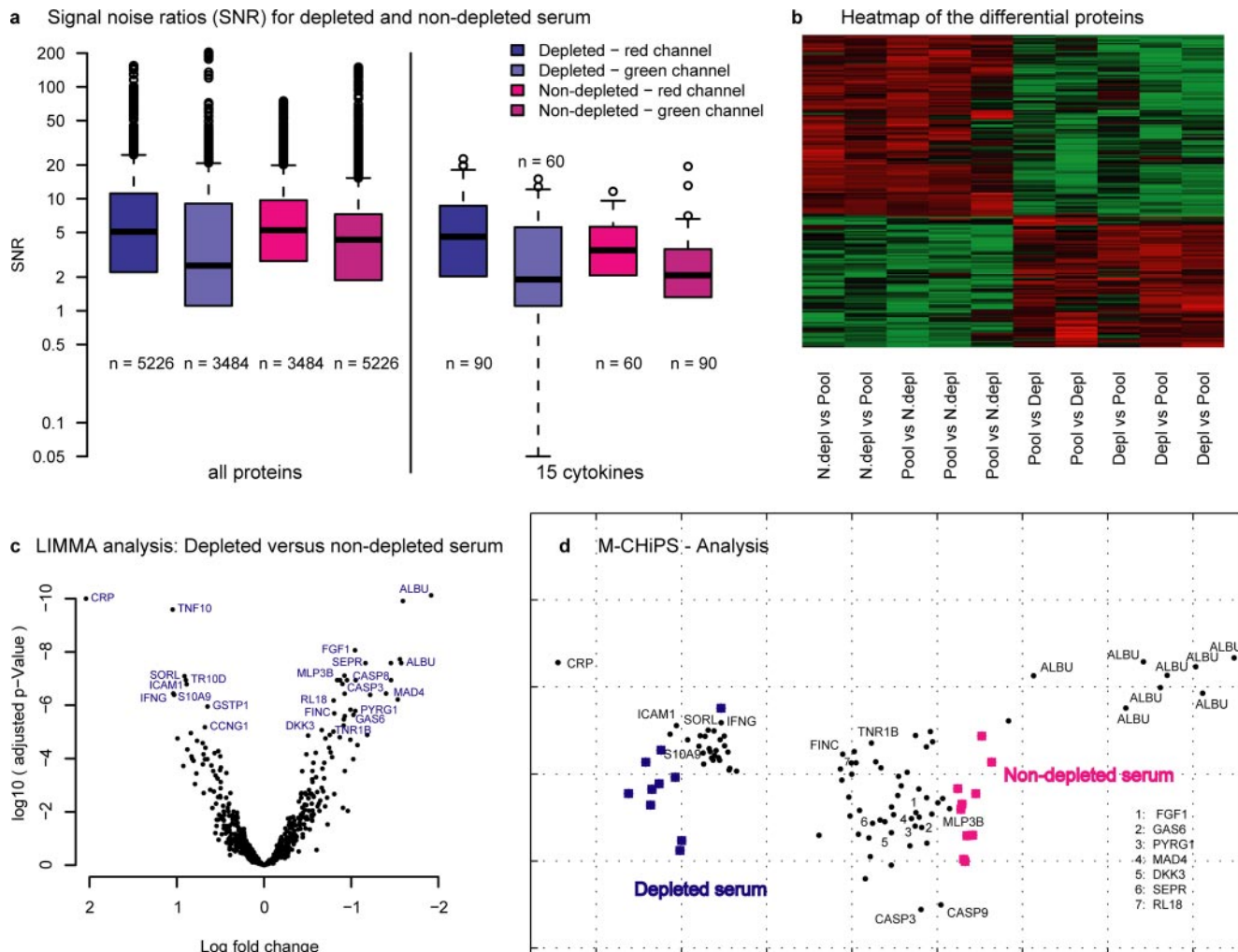


FIG. 4. **Influence of serum depletion.** a, SNRs obtained for depleted and nondepleted serum samples: the data are derived from five array measurements each, including dye swapping. Serum depletion improved the overall SNR for neither all the array features (*left panel*) nor a set of 15 low-abundance cytokines (*right panel*). b, heat map of the proteins that showed differential abundance between the two samples; overrepresented proteins are shown in red and under-represented proteins, in green. c, a volcano plot of LIMMA analysis represents the distribution of log-fold change and adjusted *p* values for all proteins. Besides albumin, a large set of 110 proteins was codepleted, whereas others were enriched. d, biplot of proteins and samples according to their expression profiles resulting from correspondence analysis with M-ChiPS: samples are depicted as colored squares, differentially abundant proteins as black dots. The closer the colocalization of two spots (both samples and proteins), the higher is the degree of association between them. Samples located in the same direction from the plot centroid exhibit a similar expression pattern. The further a protein is located in the same direction as a set of samples, the more specific it is.

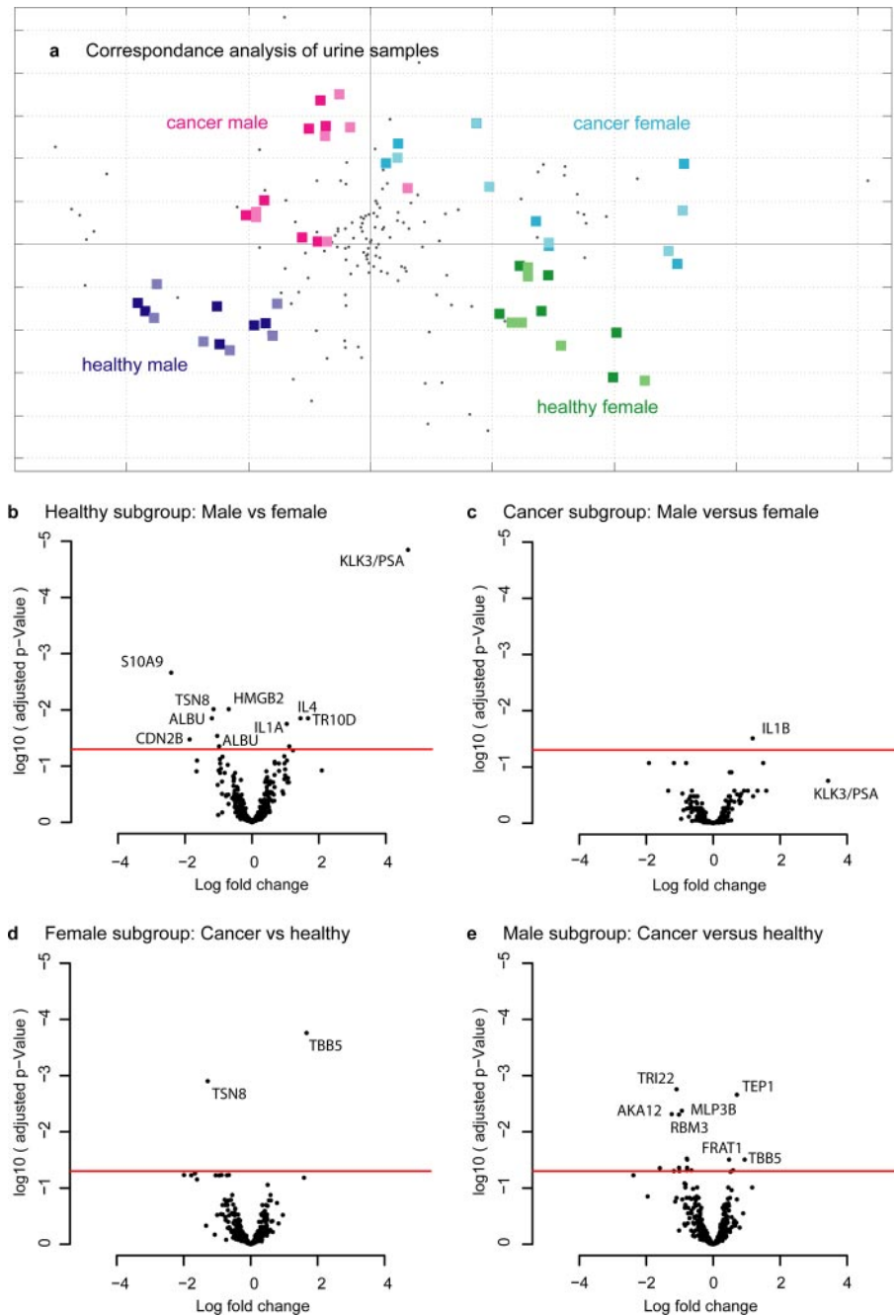
biplot (Fig. 4d), each sample is depicted as a colored square. Proteins that exhibited significantly differential levels are shown as black dots. Proteins shown on the left were enriched in the depleted sample, whereas proteins located to the right were depleted or codepleted. The results obtained with M-ChiPS match with those from the LIMMA analysis.

Pancreatic Cancer: Analyzing Urine Samples—Urine is an extremely interesting source material for biomarker screening because of its easy and noninvasive accessibility in large quantities. To verify the usability of the established antibody platform for urine protein profiling, we performed a preliminary study on 12 urine samples from six patients with

pancreatic adenocarcinoma and six healthy persons, both groups equally divided into male and female. The protein samples were labeled with Dy-549. In addition, a common reference was prepared by pooling of samples and subsequent labeling with Dy-649. In a dual-color approach, each sample was repeatedly incubated competitively with the reference. Resulting signals (e.g. Fig. 1e) had equally good or better signal-to-noise ratios than in plasma or serum incubations (Fig. 1d).

In correspondence analysis, the samples clustered in four distinct groups according to sex (horizontal axis = primary component) and disease status (vertical axis = secondary component) (Fig. 5a). Samples from male and female subjects

FIG. 5. Profiling the urine proteome of patients with pancreatic adenocarcinoma and healthy controls. *a*, correspondence analysis resulted in a biplot of differentially abundant proteins and the samples. Samples are depicted as squares that are colored according to disease state and sex; black spots represent differentially expressed proteins. Each sample is represented by four measurements representing the incubations on two arrays as well as two intra-array replicates. Measurements located in the same direction from the centroid of the plot exhibit a similar expression pattern. The smaller the distance between two samples, the higher is the concordance of their expression profiles. In addition to the more gradual variations, proteins were found that are particularly associated with the different sample groups. This association is indicated in the correspondence analysis plot by localization in the same direction off the centroid as the respective sample type; the further the distance to the centroid, the better is the correlation. One protein (KLK3) could not be displayed in the graph because it is located outside of the plotting region to the left, very strongly differentiating the male from the female samples. *b–e*, volcano plots summarize the results of LIMMA analyses. The log-fold changes and adjusted p values are shown for the sex-specific comparisons of the healthy (*b*) and diseased (*c*) subgroups as well as the disease-specific comparisons of the female (*d*) and male (*e*) subgroups. The red line marks a significance level of $p = 0.05$.



of the healthy subgroups are clearly separated, whereas there is a partial overlap between the cancer subgroups. Using LIMMA analysis, we found 11 proteins at differential levels between healthy male and female subjects at a significance level of $p < 0.05$ (Fig. 5*b*), the most prominent one being Kallikrein-3 (KLK3, also known as prostate-specific antigen; $p = 10^{-5}$; supplemental Fig. 3). In the cancer subgroup, only one protein varied between the sexes (Fig. 5*c*). In separate comparisons of the two sexes, we found two proteins (Fig. 5*d*) that differ between healthy and diseased female subjects, whereas 17 proteins showed significantly differential levels

within the male subgroup (Fig. 5*e*). The differential proteins are listed in supplemental Tables 2–5).

DISCUSSION

We established the means and quality measures for performing microarray-based, dual-color measurements of protein levels at a high level of robustness, accuracy, and reproducibility. The processes were applied to an array with a relatively high number of antibodies, specifically targeting proteins regulated in human cancers. Because of the direct labeling process (27), the array complexity will be scaled up

and expanded without major changes to the assay parameters or characteristics. In principle, the only technical limitation is the availability of well-characterized antibodies. Several initiatives exist for producing high-quality capture molecules against all human proteins (28, 29). In addition, quality standards for available antibodies are being defined to improve performance (28–31). Binders of better specificity, affinity, and stability will significantly enhance assay performance, making it possible to advance beyond the current average interarray CV of 9–14%. We obtained these values as a quality measure for all 1,800 array features without any filtering and without averaging of replicate spots. Less than 5% of the antibodies exhibited a CV >20%. In future, they could be replaced to further improve assay characteristics. Other studies reported interarray CV values of 12–22% on smaller antibody microarrays after data filtering and averaging up to eight intra-array replicates (32, 33). For a bead-based assay of 18 cytokines, a CV of 18–44% was reported (34), and for repeated mass spectrometry experiments, a CV of approximately 21% was calculated (35, 36). Our values are similar to the quality (CV of 5–15%) reported for commercial DNA-microarray platforms by the Microarray Quality Consortium (37).

An important factor to pave the way for such robust measurements has been the implementation of a dual-color assay, as demonstrated by the direct comparison of repeated one-color and dual-color mode measurements. For robust profiling, the concordance of the two color channels is an important aspect. We observed no significant dye bias for any of the studied proteins but one (ACTB), indicating that no significant dye bias is introduced by dual-color mode measurements. The results obtained with ACTB, however, demonstrate that, apart from experimental controls such as dye swap and a common reference, it is important to examine dye specificities in any proteomic assay based on labeling.

Sample preparation is even more critical for preventing experimental bias. This encompasses basic facets of protein isolation and other aspects such as protein depletion, which is commonly used in proteomic techniques to increase sensitivity (38, 39), including antibody microarrays studies (40, 41). In our experiments, serum depletion did not improve the overall sensitivity of antibody microarray detection. Instead, it had a major impact on the protein composition by affecting signal intensities of more than a quarter of the studied proteins. As reported before for other systems (42, 43), depletion of highly abundant proteins led to co-depletion of other proteins. In a mass spectrometry-based analysis, 814 proteins were identified to be codepleted with albumin and 2,091 with immunoglobulins from human plasma (44). Such major changes could obscure protein differences that occur in the original samples or introduce them artificially. Depletion seems to be disadvantageous for experiments with direct sample labeling (27) and optimized incubation conditions (11). Antibody microar-

rays have the intrinsic advantage that proteins are captured on a solid support. By the enrichment at a particular location, they become detectable even at low abundance (11, 45). In addition, the presence of high-molecular-weight proteins such as albumin or immunoglobulins could even have a favorable effect by shielding other proteins from accumulating at the array surface. Primarily large and highly abundant proteins are interacting with the surface, which can be removed in washing steps more efficiently. In consequence, small, low-abundant proteins remain in solution and are thus more likely to bind to the capture agents.

Because antibody microarrays do not require protein depletion or the removal of lipids for plasma or serum samples, they facilitate profiling studies as they are usually performed on clinical samples. Therefore, it should be possible to transfer biomarkers obtained by antibody microarray studies more easily and quickly into other immuno-based assay formats for clinical validation.

The small pilot study on identifying pancreatic cancer with an analysis of urine samples clearly indicated the technique's potential for diagnosis. We could unambiguously differentiate between those subjects with pancreatic cancer and healthy control subjects. Similar results were obtained before for serum samples in two different studies using antibody microarray targeting approximately 60 different proteins (32, 46). Besides the disease-specific grouping, we were able to distinguish samples according to gender, which has also been observed in mass spectrometry analysis.² KLK3 exhibited the strongest discrimination power in the healthy subgroup. KLK3, usually referred to as prostate specific antigen, is known to be primarily found in males. In the analysis, other proteins have been identified that discriminate with high significance between the patients with cancer and the healthy individuals included in the assay. As in the previous studies on serum samples, the data need to be confirmed on a larger study cohort, taking into account additional and critical controls such as pancreatitis and obstructive jaundice (47), before any clinically relevant conclusions can be drawn. An important finding, however, is the fact that proteins that exhibited cancer-specific regulation were highly diverse between the male and the female subgroups. This may underline the importance of a gender-specific scheme of biomarker identification.

In summary, we demonstrated the reliable and reproducible application of antibody microarrays in a two-color mode for human plasma and serum samples as well as urine. The ability to discriminate between patients with cancer and healthy subjects with still relatively few albeit carefully selected antibodies and with a small number of protein samples demonstrates the enormous potential of high-content antibody microarrays, which will be one of the results of the ongoing quest for comprehensive sets of highly reliable antibodies.

² T. Crnogorac-Jurcevic, unpublished data.

Such an immuno-based platform and the ability to apply clinical samples without major preparative steps in a robust and highly parallel manner may assist the technology's rapid clinical application.

Acknowledgments—We are grateful to T. Gress, F. Diehl, and M. Nees for contributions to the selection of target proteins. Early contributions of W. Kusnezow to antibody attachment and incubation conditions are gratefully acknowledged. A set of 668 antibodies was created by the company Eurogentec (Seraing, Belgium) and provided on a complimentary basis.

* This work was supported in part by the European Commission in the MolTools, DropTop, and MolDiagPaca projects.

☐ This article contains supplemental Figs. 1–3 and supplemental Tables 1–5.

§ Supported by a stipend of the International Ph.D. program of Deutsches Krebsforschungszentrum. To whom correspondence should be addressed: Im Neuenheimer Feld 580, D-69120 Heidelberg, Germany. Tel.: 49-6221-424685; Fax: 49-6221-424689; E-mail: christoph.schroeder@dkfz.de.

REFERENCES

- Hanash, S. M., Pitteri, S. J., and Faca, V. M. (2008) Mining the plasma proteome for cancer biomarkers. *Nature* **452**, 571–579
- Zhao, Y., Lee, W. N., and Xiao, G. G. (2009) Quantitative proteomics and biomarker discovery in human cancer. *Expert Rev. Proteomics* **6**, 115–118
- Koomen, J. M., Haura, E. B., Bepler, G., Sutphen, R., Remily-Wood, E. R., Benson, K., Hussein, M., Hazlehurst, L. A., Yeatman, T. J., Hildreth, L. T., Sellers, T. A., Jacobsen, P. B., Fenstermacher, D. A., and Dalton, W. S. (2008) Proteomic contributions to personalized cancer care. *Mol. Cell. Proteomics* **7**, 1780–1794
- Ghosh, D., and Poisson, L. M. (2009) “Omics” data and levels of evidence for biomarker discovery. *Genomics* **93**, 13–16
- Mischak, H., Apweiler, R., Banks, R. E., Conaway, M., Coon, J., Dominiczak, A., Ehrlich, J. H. H., Fliser, D., Girolami, M., Hermjakob, H., Hochstrasser, D., Jankowski, J., Julian, B. A., Kolch, W., Massy, Z. A., Nesuess, C., Novak, J., Peter, K., Rossing, K., Schanstra, J., Semmes, O. J., Theodorescu, D., Thongboonkerd, V., Weissinger, E. M., Eyk, J. E. V., and Yamamoto, T. (2007) Clinical proteomics: A need to define the field and to begin to set adequate standards. *Proteomics Clin. Appl.* **1**, 148–156
- Beretta, L. (2007) Proteomics from the clinical perspective: many hopes and much debate. *Nat. Methods* **4**, 785–786
- Borrebaeck, C. A., and Wingren, C. (2009) Transferring proteomic discoveries into clinical practice. *Expert Rev. Proteomics* **6**, 11–13
- Sanchez-Carbayo, M. (2006) Antibody arrays: technical considerations and clinical applications in cancer. *Clin. Chem.* **52**, 1651–1659
- Loch, C. M., Ramirez, A. B., Liu, Y., Sather, C. L., Delrow, J. J., Scholler, N., Garvik, B. M., Urban, N. D., McIntosh, M. W., and Lampe, P. D. (2007) Use of high density antibody arrays to validate and discover cancer serum biomarkers. *Mol. Oncol.* **1**, 313–320
- Alhamedani, M. S., Schröder, C., and Hoheisel, J. D. (2009) Oncoproteomic profiling with antibody microarrays. *Genome Med.* **1**, 68
- Kusnezow, W., Syagailo, Y. V., Ruffer, S., Baudenstiel, N., Gauer, C., Hoheisel, J. D., Wild, D., and Goychuk, I. (2006) Optimal design of microarray immunoassays to compensate for kinetic limitations: theory and experiment. *Mol. Cell. Proteomics* **5**, 1681–1696
- Wingren, C., Ingvarsson, J., Dexlin, L., Szul, D., and Borrebaeck, C. A. K. (2007) Design of recombinant antibody microarrays for complex proteome analysis: Choice of sample labeling-tag and solid support. *Proteomics* **7**, 3055–3065
- Borrebaeck, C. A., and Wingren, C. (2009) Design of high-density antibody microarrays for disease proteomics: Key technological issues. *J. Proteomics* **72**, 928–935
- Bauer, A., Kleeff, J., Bier, M., Wirtz, M., Kayed, H., Esposito, I., Korc, M., Hafner, M., Hoheisel, J. D., and Friess, H. (2009) Identification of malignancy factors by analyzing cystic tumors of the pancreas. *Pancreatology* **9**, 34–44
- Buchholz, M., Kestler, H. A., Bauer, A., Böck, W., Rau, B., Leder, G., Kratzer, W., Bommer, M., Scarpa, A., Schilling, M. K., Adler, G., Hoheisel, J. D., and Gress, T. M. (2005) Specialized DNA arrays for the differentiation of pancreatic tumors. *Clin. Cancer Res.* **11**, 8048–8054
- Notterman, D. A., Alon, U., Sierk, A. J., and Levine, A. J. (2001) Transcriptional gene expression profiles of colorectal adenoma, adenocarcinoma, and normal tissue examined by oligonucleotide arrays. *Cancer Res.* **61**, 3124–3130
- Cham, B. E., and Knowles, B. R. (1976) A solvent system for delipidation of plasma or serum without protein precipitation. *J. Lipid Res.* **17**, 176–181
- Tonack, S., Aspinall-O'Dea, M., Jenkins, R. E., Elliot, V., Murray, S., Lane, C. S., Kitteringham, N. R., Neoptolemos, J. P., and Costello, E. (2009) A technically detailed and pragmatic protocol for quantitative serum proteomics using iTRAQ. *J. Proteomics* **73**, 352–356
- Weeks, M. E., Hariharan, D., Petronijevic, L., Radon, T. P., Whiteman, H. J., Kocher, H. M., Timms, J. F., Lemoine, N. R., and Crnogorac-Jurcevic, T. (2008) Analysis of the urine proteome in patients with pancreatic ductal adenocarcinoma. *Proteomics Clin. Appl.* **2**, 1047–1057
- Smyth, G. K. (2004) Linear models and empirical Bayes methods for assessing differential expression in microarray experiments. *Stat. Appl. Genet. Mol. Biol.* **3**, article 3
- Ritchie, M. E., Silver, J., Oshlack, A., Holmes, M., Diyagama, D., Holloway, A., and Smyth, G. K. (2007) A comparison of background correction methods for two-colour microarrays. *Bioinformatics* **23**, 2700–2707
- Smyth, G. K., and Speed, T. (2003) Normalization of cDNA microarray data. *Methods* **31**, 265–273
- Smyth, G. K., Michaud, J., and Scott, H. S. (2005) Use of within-array replicate spots for assessing differential expression in microarray experiments. *Bioinformatics* **21**, 2067–2075
- Benjamini, Y., and Hochberg, Y. (1995) Controlling the false discovery rate: A practical and powerful approach to multiple testing. *J. R. Stat. Soc. B* **57**, 289–300
- Fellenberg, K., Hauser, N. C., Brors, B., Neutzner, A., Hoheisel, J. D., and Vingron, M. (2001) Correspondence analysis applied to microarray data. *Proc. Natl. Acad. Sci. U. S. A.* **98**, 10781–10786
- Fellenberg, K., Busold, C. H., Witt, O., Bauer, A., Beckmann, B., Hauser, N. C., Frohme, M., Winter, S., Dippon, J., and Hoheisel, J. D. (2006) Systematic interpretation of microarray data using experiment annotations. *BMC Genomics* **7**, 319
- Kusnezow, W., Banzon, V., Schröder, C., Schaal, R., Hoheisel, J. D., Ruffer, S., Luft, P., Duschl, A., and Syagailo, Y. V. (2007) Antibody microarray-based profiling of complex specimens: Systematic evaluation of labeling strategies. *Proteomics* **7**, 1786–1799
- Nilsson, P., Paavilainen, L., Larsson, K., Odling, J., Sundberg, M., Andersson, A. C., Kampf, C., Persson, A., Al-Khallil, Szigyarto, C., Ottosson, J., Björling, E., Hober, S., Wernérus, H., Wester, K., Pontén, F., and Uhlen, M. (2005) Towards a human proteome atlas: High-throughput generation of mono-specific antibodies for tissue profiling. *Proteomics* **5**, 4327–4337
- Taussig, M. J., Stoevesandt, O., Borrebaeck, C. A., Bradbury, A. R., Cahill, D., Cambillau, C., de Daruvar, A., Dübel, S., Eichler, J., Frank, R., Gibson, T. J., Gloriam, D., Gold, L., Herberg, F. W., Hermjakob, H., Hoheisel, J. D., Joos, T. O., Kallioniemi, O., Koegl, M., Koegl, M., Konthur, Z., Korn, B., Kremmer, E., Krobitch, S., Landegren, U., van der Maarel, S., McCafferty, J., Muylidermans, S., Nygren, P. A., Palcy, S., Plückthun, A., Polic, B., Przybylski, M., Saviranta, P., Sawyer, A., Sherman, D. J., Skerra, A., Templin, M., Ueffing, M., and Uhlen, M. (2007) ProteomeBinders: Planning a European resource of affinity reagents for analysis of the human proteome. *Nat. Methods* **4**, 13–17
- Blow, N. (2007) Antibodies: The generation game. *Nature* **447**, 741–744
- Björling, E., and Uhlen, M. (2008) Antibodypedia, a portal for sharing antibody and antigen validation data. *Mol. Cell. Proteomics* **7**, 2028–2037
- Orchekowski, R., Hamelinck, D., Li, L., Gliwa, E., vanBrocklin, M., Marrero, J. A., Van de Woude, G. F., Feng, Z., Brand, R., and Haab, B. B. (2005) Antibody microarray profiling reveals individual and combined serum proteins associated with pancreatic cancer. *Cancer Res.* **65**, 11193–11202
- Hamelinck, D., Zhou, H., Li, L., Verweij, C., Dillon, D., Feng, Z., Costa, J.,

- and Haab, B. B. (2005) Optimized normalization for antibody microarrays and application to serum-protein profiling. *Mol. Cell. Proteomics* **4**, 773–784
34. Wong, H. L., Pfeiffer, R. M., Fears, T. R., Vermeulen, R., Ji, S., and Rabkin, C. S. (2008) Reproducibility and correlations of multiplex cytokine levels in asymptomatic persons. *Cancer Epidemiol. Biomarkers Prev.* **17**, 3450–3456
 35. Levin, Y., Wang, L., Ingudomnukul, E., Schwarz, E., Baron-Cohen, S., Palotás, A., and Bahn, S. (2009) Real-time evaluation of experimental variation in large-scale LC-MS/MS-based quantitative proteomics of complex samples. *J. Chromatogr. B Analyt. Technol. Biomed. Life Sci.* **877**, 1299–1305
 36. Neubert, H., Bonnert, T. P., Rumpel, K., Hunt, B. T., Henle, E. S., and James, I. T. (2008) Label-free detection of differential protein expression by LC/MALDI mass spectrometry. *J. Proteome Res.* **7**, 2270–2279
 37. Shi, L., Reid, L. H., Jones, W. D., Shippy, R., Warrington, J. A., Baker, S. C., Collins, P. J., de Longueville, F., Kawasaki, E. S., Lee, K. Y., Luo, Y., Sun, Y. A., Willey, J. C., Setterquist, R. A., Fischer, G. M., Tong, W., Dragan, Y. P., Dix, D. J., Frueh, F. W., Goodsaid, F. M., Herman, D., Jensen, R. V., Johnson, C. D., Lobenhofer, E. K., Puri, R. K., Schrf, U., Thierry-Mieg, J., Wang, C., Wilson, M., Wolber, P. K., Zhang, L., Amur, S., Bao, W., Barbacioru, C. C., Lucas, A. B., Bertholet, V., Boysen, C., Bromley, B., Brown, D., Brunner, A., Canales, R., Cao, X. M., Cebula, T. A., Chen, J. J., Cheng, J., Chu, T. M., Chudin, E., Corson, J., Corton, J. C., Croner, L. J., Davies, C., Davison, T. S., Delenstarr, G., Deng, X., Dorris, D., Eklund, A. C., Fan, X. H., Fang, H., Fulmer-Smentek, S., Fuscoe, J. C., Gallagher, K., Ge, W., Guo, L., Guo, X., Hager, J., Haje, P. K., Han, J., Han, T., Harbottle, H. C., Harris, S. C., Hatchwell, E., Hauser, C. A., Hester, S., Hong, H., Hurban, P., Jackson, S. A., Ji, H., Knight, C. R., Kuo, W. P., LeClerc, J. E., Levy, S., Li, Q. Z., Liu, C., Liu, Y., Lombardi, M. J., Ma, Y., Magnuson, S. R., Maqsodi, B., McDaniel, T., Mei, N., Myklebost, O., Ning, B., Novorodovskaya, N., Orr, M. S., Osborn, T. W., Papallo, A., Patterson, T. A., Perkins, R. G., Peters, E. H., Peterson, R., Phillips, K. L., Pine, P. S., Pusztai, L., Qian, F., Ren, H., Rosen, M., Rosenzweig, B. A., Samaha, R. R., Schena, M., Schroth, G. P., Shchegrova, S., Smith, D. D., Staedtler, F., Su, Z., Sun, H., Szallasi, Z., Tezak, Z., Thierry-Mieg, D., Thompson, K. L., Tikhonova, I., Turpaz, Y., Vallanat, B., Van, C., Walker, S. J., Wang, S. J., Wang, Y., Wolfinger, R., Wong, A., Wu, J., Xiao, C., Xie, Q., Xu, J., Yang, W., Zhang, L., Zhong, S., Zong, Y., and Slikker, W., Jr. (2006) The MicroArray Quality Control (MAQC) project shows inter- and intraplatform reproducibility of gene expression measurements. *Nat. Biotechnol.* **24**, 1151–1161
 38. Fountoulakis, M., Juranville, J. F., Jiang, L., Avila, D., Röder, D., Jakob, P., Berndt, P., Evers, S., and Langen, H. (2004) Depletion of the high-abundance plasma proteins. *Amino Acids* **27**, 249–259
 39. de Roos, B., Duthie, S. J., Polley, A. C., Mulholland, F., Bouwman, F. G., Heim, C., Rucklidge, G. J., Johnson, I. T., Mariman, E. C., Daniel, H., and Elliott, R. M. (2008) Proteomic methodological recommendations for studies involving human plasma, platelets, and peripheral blood mononuclear cells. *J. Proteome Res.* **7**, 2280–2290
 40. Ingvarsson, J., Lindstedt, M., Borrebaeck, C. A., and Wingren, C. (2006) One-step fractionation of complex proteomes enables detection of low abundant analytes using antibody-based microarrays. *J. Proteome Res.* **5**, 170–176
 41. Desrosiers, R. R., Beaulieu, E., Buchanan, M., and Béliveau, R. (2007) Proteomic analysis of human plasma proteins by two-dimensional gel electrophoresis and by antibody arrays following depletion of high-abundance proteins. *Cell Biochem. Biophys.* **49**, 182–195
 42. Granger, J., Siddiqui, J., Copeland, S., and Remick, D. (2005) Albumin depletion of human plasma also removes low abundance proteins including the cytokines. *Proteomics* **5**, 4713–4718
 43. Gundry, R. L., White, M. Y., Noguee, J., Tchernyshyov, I., and Van Eyk, J. E. (2009) Assessment of albumin removal from an immunoaffinity spin column: Critical implications for proteomic examination of the albuminome and albumin-depleted samples. *Proteomics* **9**, 2021–2028
 44. Shen, Y., Kim, J., Strittmatter, E. F., Jacobs, J. M., Camp, D. G., 2nd, Fang, R., Tolié, N., Moore, R. J., and Smith, R. D. (2005) Characterization of the human blood plasma proteome. *Proteomics* **5**, 4034–4045
 45. Ekins, R. P. (1998) Ligand assays: from electrophoresis to miniaturized microarrays. *Clin. Chem.* **44**, 2015–2030
 46. Ingvarsson, J., Wingren, C., Carlsson, A., Ellmark, P., Wahren, B., Engström G., Harmenberg, U., Krogh, M., Peterson, C., and Borrebaeck, C. A. (2008) Detection of pancreatic cancer using antibody microarray-based serum protein profiling. *Proteomics* **8**, 2211–2219
 47. Yan, L., Tonack, S., Smith, R., Dodd, S., Jenkins, R. E., Kitteringham, N., Greenhalf, W., Ghaneh, P., Neoptolemos, J. P., and Costello, E. (2009) Confounding effect of obstructive jaundice in the interpretation of proteomic plasma profiling data for pancreatic cancer. *J. Proteome Res.* **8**, 142–148